doi.org/10.36721/PJPS.2026.39.4.REG.14614.1

Precise thrombolysis *in-vivo* and *in-vitro* study on improved MnO_2-loaded pep'-Fuco nanocarriers

Dongyan Yin[1], Yuqi Bai[2]*, Ying Wang[1], Cuiping Zhao[1], Xiaodong Xiao[1] and Tongtong Li[1]
[1]School of Medicine, Zhengzhou University of Industrial Technology, Xinzheng, China.
[2]The Third Department of Internal Medicine, Xindian Central Health Center, Xinzheng, Xinzheng, China.

Abstract: **Background**: Venous thrombosis is the main cause of incidence rate and mortality of cardiovascular diseases worldwide. The current thrombolytic therapy often faces systemic side effects, limited targeting, and adverse hypoxic microenvironment adjustments within the thrombus, which may impair efficacy. **Objective**: The goal is to investigate the thrombolytic effect of MnO2@pep'-Fuco needle on venous thrombosis in both *in-vivo* and *in-vitro* environments. **Methods**: In this study, we have injected rats with PBS, MnO2@pep-Fuco, free uPA, MnO2-COOH/uPA, MnO2/uPA@pep-Fuco and MnO2/uPA@pep'-Fuco and then we have measured their vascular occlusion rate, haemolysis, body weight and the biochemical profile of plasma. **Results**: The study systematically evaluates the thrombolytic performance of MnO2@pep'-Fuco nanoparticles and it is observed that these flower-shaped nanoparticles have a pep-Fuco grafting rate of 3.87%. They can release 23.2% of dissolved oxygen within 25 minutes and achieve 90.5% drug release rate within 50 hours. The nanoparticles also exhibit excellent biocompatibility, with a cell death rate of 1.26% and red blood cell adhesion rate of 90%. *In-vivo* experiments, a complete thrombolysis (100%) has been achieved with a thrombus-to-vein fluorescence intensity ratio of 2:7. The study reveals excellent biosafety, with a hemolysis rate of 0.65 to 0.82% without any significant changes in body weight. **Conclusion**: These results indicate that the MnO2/uPA@pep-Fuco nanoparticle system is a promising novel therapeutic strategy for treating venous thrombosis with great efficacy.

Keywords: Intravenous thrombolysis; MnO_2; Nanocarriers; Thrombin; Urokinase; Venous thrombosis

Submitted on 20-05-2025 – Revised on 19-09-2025 – Accepted on 09-10-2025

INTRODUCTION

With the changes in fast-paced lifestyle of human beings, physical diseases are gradually increasing. In the current era, a few diseases are growing rapidly such as cardiovascular diseases (CVD), brain strokes and cancers. The incidence of CVD is growing in the young population as well. Venous thrombosis is observed as the root cause of CVD, which is getting attention from researchers and doctors (Schmitt *et al*., 2022). To investigate the influencing factors of post thrombotic syndrome caused by venous thrombosis, the researchers (Li *et al*., 2021) have conducted relevant experiments to analyze the time window limitations of post thrombotic syndrome. The research results reveal that the thrombus burden and venous wall fibrosis are alleviated on day 8 in the experimental mice connected to the blood flow catheter, with a difference of 8.41 from the initial level. Therefore, within a limited time window, blood flow catheters can effectively improve the diagnostic resolution of post thrombotic syndrome. The authors in another study have taken 5497 subjects with venous thrombosis at a hospital in the United States for similar study. Their study includes 2688 cases of pulmonary embolism and 1625 cases of lower limb thrombosis. The study shows that 4.5% of patients have lost their lives at the onset of the disease and 15.4% of patients lost their lives within the next three months (Fang *et al*., 2020). Afifi *et al*. have conducted a study on intracranial hemorrhage caused by venous thrombosis. The study considers 260 subjects and evaluates the clot burden by counting the number of venous sinuses and veins formed by thrombosis on confirmatory imaging to analyze the occurrence of intracranial hemorrhage. The outcomes reveal that the proportion of minor subcortical bleeding is 29%, subarachnoid hemorrhage is 24%, subdural hemorrhage is 11% and 23% is contributed by concurrent bleeding. Therefore, intracranial hemorrhage has higher incidence in venous thrombosis (Afifi *et al*., 2020). It indicates that venous thrombosis has significant adverse effects on human health. To effectively treat venous thrombosis, many researchers have proposed different methods for diagnosis and treatment. Powell *et al*. conducts anticoagulant therapy with low molecular weight heparin for 12 months to control the formation of venous thrombosis. This study explores the occurrence and physiological phenomena of thrombosis during treatment and analyzed the treatment status of low molecular weight heparin. The research results indicate that the highest risk of recurrence of thrombotic events is 11.2% for patients treated with low molecular weight heparin, respectively. Therefore, this drug has anti-thrombotic effect (Powell *et al*., 2021). Albertsen *et al*. have proposed the usage of rivaroxaban and apixaban for the treatment of high recurrence of venous thrombosis. After setting up different control experiments, the experimental results show that the probability of pulmonary embolism

*Corresponding authors: e-mails: bai5178321881@163.com

symptoms is related to the dosage of medication and only a small number of patients received extended treatment, while the rest of patients could recover during the experimental treatment period (Albertsen *et al*., 2021). Nanodrugs are a form of medication that makes use of nanotechnology to prepare drugs and these drugs not only have good targeting ability, but also have high biocompatibility (Zajdel *et al*., 2021).

Therefore, the proposed study uses nano drugs for thrombolytic therapy of venous thrombosis. It uses nano preparation technology to prepare flower shaped manganese dioxide nanoparticles (MnO_2) and then combines fucose (Fuco) and thrombin peptides (pep) as targeting agents. Thrombolytic drugs have been administered using urokinase (uPA) to treat CVD. This study considers thrombolytic performance of the system in both in-vivo and in- vitro environments. This article is structured into four parts. The first section presents background details and a review of the existing research studies and also states the research contributions of this article. The second part elaborates the research on the thrombolytic performance methods of MnO_2@pep'-Fuco (MPF) nano drug delivery systems. The third part provides the performance analysis of the proposed study. The fourth part presents the summary of the research and limitations of the study.

MATERIALS AND METHODS

Study on improving the thrombolytic performance of MPF nanocarriers

Due to the high risk of massive bleeding during the treatment of venous thrombosis, attention needs to be paid to the hemolysis and hemostatic effect of nano drug delivery systems in venous blood during thrombolytic therapy. To provide precise thrombolytic therapy for venous thrombosis, this study proposes the preparation of a novel MPF material as a carrier for uPA to form MAF delivery system. This study conducts an experimental design to determine the in-vitro and in-vivo thrombolysis ability of the system to verify the effectiveness of the nanosystem.

Instruments and reagents

The preparation of MPF nanocarriers in this study is divided into three parts. It begins with the preparation of MnO_2 nanoparticles. Then, the preparation of pep-Fuco composite compounds takes place, followed by the preparation of MPF nanomaterials. Finally, the preparation of the MAF delivery system takes place. The required instruments and reagents for the preparation experiment of the above materials are as follows: Ultra-pure water apparatus, heating Magnetic Stirrer, benchtop centrifuge, ultrasonic cleaner, muffle furnace, pH meter, portable dissolved oxygen meter, Fourier Transform Infrared (FTIR) spectrometer, fluorescence spectrophotometer, transmission electron microscope, X-ray diffractometer, scanning electron microscope and fluorescence microscope. The reagents required for the preparation and characterization of the above materials are potassium bromide, sodium dodecylbenzene sulfonate, carbamide, potassium permanganate, 3-Aminopropyltriethoxysilane, N-Dimethylformamide, 4-Dimethylaminopyridine, triethylamine, polypeptide, chain of amino acids linked by peptide bonds CO-NH, Fucoidan, urokinase (enzyme), Thrombin, Carboxamide, 2,4,6-Trichlorobenzoyl chloride, 1-(3-Dimethylaminopropyl)-3-ethylcarbodiimide hydrochloride, N-Hydroxysuccinimide, dimethyl sulfoxide and Fluorescein isothiocyanate The preparation and characterization of the nanocarriers required for this study can be carried out using the equipment and the reagents listed in the above paragraphs.

Preparation of MnO_2/uPA@pep-Fuco nanodelivery system

The MnO_2 nanoparticles in this study are synthesized using a template method. First, 3.484g of Sodium Dodecyl Benzene Sulfonate (SDBS) solid powder is mixed with 20mL of ultrapure water. (Zhou, J., *et al*. 2019) Then the beaker is placed in a 75°C oil bath for magnetic stirring, with a stirring time of 10 minutes. Then it weighs 0.1486g of $KMnO_4$ particles into a beaker containing 10mL of ultrapure water, it places the beaker in an ultrasonic instrument and sonicates at 25 °C for 30 minutes. It adds $KMnO_4$ solution to the stirred SDBS solution and stirs in an oil bath at 75 °C for 15 minutes (Abasian *et al*., 2021; Zhou *et al*., 2019). The mixed solution system after uniform stirring appears purple red. It then adds a 4mL/L nitric acid solution dropwise to the aforementioned mixed solution. When the color of the mixed solution changes to light purple, the operation is stopped. The mixed solution is added to an oil bath at 75°C and continues to stir until the purple disappears completely and white foam floats on the upper layer of the solution. It centrifuges the solution at 13000 rpm for 10 minutes. The precipitate after centrifugation is first washed three times with ultrapure water and anhydrous ethanol. Then it is placed in a dialysis bag and the specifications of the molecular weight cut off (MWCO) of the dialysis bag is equal to 3.5 kDa

This study uses dialysis bags with the specifications to obtain residual solids and then dries the residual solids in a dryer at 100°C for 8 hours to obtain flower shaped mesoporous MnO_2 nanoparticles. It then weighs 45mg of flower shaped mesoporous MnO_2 nanoparticles and sonicated in 20mL of anhydrous ethanol for 30 minutes. 230μL3-aminopropyltriethoxysilane and 1.5mL of ultrapure water are added and stirs at 45°C for 12 hours (Xu *et al*., 2019; Miao *et al*., 2022). Afterwards, the precipitate obtained by centrifugation is washed three times with anhydrous ethanol and dried at 55°C to obtain MnO_2-NH_2 nanoparticles. Then, 50mg of MnO_2-NH_2 nanoparticles are weighed, added to 12mL of

dimethylformamide and sonicated, followed by 95mg of succinic anhydride, 55mg of DMAP and 135μL of triethylamine, stirred evenly and centrifuged. After centrifugation and precipitation at 50°C for drying, MnO_2-COOH (MCO) was obtained.

The main instrument models, brands, and sources used in the study are as follows: Milli-Q ultrapure water analyzer (Integral, Merck Millipore), Heating Magnetic Stirrer (IKA) ®RCT, IKA), Desktop centrifuge (Eppendorf 5425R, Eppendorf), scanning electron microscope (SU8010, Hitachi), transmission electron microscope (JEM-1400Plus, JEOL), FTIR spectrometer (Nicolet iS5, Thermo Fisher Scientific), enzyme-linked immunosorbent assay (ELISA) reader (Synergy H1, BioTek). The key chemical sources used in the experiment include potassium permanganate APTES, Urokinase (uPA) and thrombin were purchased from Sigma Aldrich; Fucoidan and synthetic peptides are derived from Sigma Aldrich and Gill Biochemistry, respectively; The BCA protein quantification kit was purchased from Beyotime Biotechnology; The experimental animal C57BL/6J mice were provided by Beijing Weitonglihua or Jackson Laboratory.

Potassium permanganate, sodium dodecylbenzenesulfonate, 3-aminopropyltriethoxysilane, urokinase and thrombin were all purchased from Sigma Aldrich; The fucoidan was purchased from Sigma Aldrich; Specific peptides are provided by Gill Biochemistry; EDC·HCl and NHS from Sigma Aldrich; 2,4,6-trichlorobenzoyl chloride and succinic anhydride were purchased from TCI; The BCA protein detection kit is sourced from Beyotime Biotechnology; The fetal bovine serum and culture medium used for cell culture were obtained from Gibco (Thermo Fisher Scientific); Fluorescent dyes such as Calcein AM, propidium iodide, and Hoechst 33342 are supplied by MedChemExpress.

Preparation of pep Fuco composite compound

The molecular sieve is dried up initially at 260°C for 5 hours and then formamide is added to it after cooling at room temperature. Then 35mg of peptides is dissolved in 10mL of formamide and sequentially 75μL of 2,4,6-trichlorobenzoyl chloride is added to this solution along with 85mg of DMAP and 85 μL triethylamine. The mixed solution is stirred evenly at room temperature to activate the carboxyl group of PEP.

Then, 10mg of Fuco is added to formamide at room temperature and it is placed in the dark for 24 hours (Cheng *et al*., 2021). Then it adds -20°C acetone to it and places it in a refrigerator at 4 °C for 15 minutes, followed by centrifugation at a speed of 13000 r/min. It transfers the precipitate after centrifugation to a dialysis bag and the specifications of the dialysis bag. After 24 hours of dialysis and drying, the pep Fuco (PFU) complex is obtained.

Preparation of MPF nanomaterials

Prepare 5mg MCO in MAF and mix it in 1mL PBS buffer. Then, 20.45 mg of 1-Ethyl-3-(3-dimethylaminopropyl) carbodiimide Hydrochloride (EDC*HCL) and 23.17mg of NHS are added to the mixture. After ultrasonic mixing, the carboxyl group is activated by stirring with room temperature magnetic force for 30min. (Mittal, A., *et al*. 2020). It adds NaOH solution to the activated solution and adjusts it to a pH of 7.0. Then it is added to the PFU composite and dissolved in 1mL of PBS buffer. Then it is added to the activated MCO solution and finally, thrombin is added, stirred uniformly with magnetic force and placed at room temperature for 36 hours (Lin *et al*., 2021). It centrifuges the stationary solution at a speed of 12000 r/min for 10 minutes, washes the precipitate with ultrapure water three times and dries it to obtain the MPF nano carrier.

Preparation of MAF nano delivery system

In this experiment, 1.2mg of MnO_2@pep-Fuco (MPPF) prepared in 2.2.3 is weighed and 2.5mL of PBS solution is added to it. Then, the solution is dispersed by exploring for more than 3 minutes in an ice bath. Then 1.8mg of uPA is added to 1.8mL of PBS. The uPA solution is added to the PBS solution of MPPF. After ultrasound for 2.5 hours under ice bath conditions, it is centrifuged at 13000 r/min at 4°C for 10 minutes. After drying the precipitate, MAF nano drug delivery system is obtained (Wilson *et al*., 2021; Kenry *et al*., 2021).

Characterization of MPF nano-delivery system

In this experiment, a certain amount of MnO_2 nanoparticles are selected and characterized by scanning electron microscopy (SEM) to obtain corresponding SEM characterization images of the nanoparticles.

Determination of grafting rate of PFU composite

The grafting rate of PFU composite is measured by the biuret method. The experiment first uses the bicinonic acid (BCA) method to determine the corresponding BSA curve. Then it weighs 5mg of PFU and prepares a sample solution with a concentration of 5mg/mL using PBS buffer as the solvent. Then, using PBS buffer as the blank control, the BCA working solution and sample solution are piped into a 96 well plate and the absorbance is measured at 562nm on an enzyme-linked immunosorbent assay. The grafting rate of the PFU composite is calculated according to the standard curve (Mittal *et al*., 2020; Oshiro-Júnior *et al*., 2020). The calculation formula is shown in Equation. (1).

$$J(\%) = \frac{c(pep)}{c(pep - Fuco)} \times 100\% \quad (1)$$

In Equation. (1), J is the grafting rate. $C(pep)$ is the concentration of pep. $C(pep\text{-}F\mu co)$ is the concentration of PFU. From this, the grafting rate of PFU can be calculated.

Determination of H_2O_2 like enzyme activity of MPF

This experiment uses PBS buffer to dilute 30% H_2O_2 solution to 0.2mM, 1mM and 100mM, respectively. Then, 10ml of MCO and MPPF solutions are added separately to achieve a concentration of 50μg/mL of nanoparticles. Take 10 mL of H_2O_2 solutions of various concentrations, add 10 mL of nano material dispersion (ensuring a final nano material concentration of 50 μg/mL), mix and immediately use a dissolved oxygen analyzer to seal and monitor the dynamic changes in dissolved oxygen concentration over time in the system. Quantitatively evaluate the enzymatic activity of different nanomaterials by comparing the rate of oxygen generation catalyzed by different H_2O_2 concentrations or the oxygen production at specific time points.

Determination of drug loading performance of MnO_2/uPA@pep-Fuco

Prepare corresponding MAF materials in this experiment. After centrifugation, the supernatant is transferred into a 96-well plate, with PBS serving as the blank control. It uses the BCA method to determine the corresponding free drug concentration. The formula for free drug rate of MAF is shown in Equation. (2).

$$Y(\%) = \frac{W_Y}{W_Z} \times 100\% \tag{2}$$

In Equation. (2), Y is the free drug rate. W_Y is the mass of the free drug. W_Z is the quality of the input drug. Similarly, the encapsulation efficiency of MAF can be obtained. The calculation is shown in Equation. (3).

$$B(\%) = \frac{W_S}{W_Z} \times 100\% \tag{3}$$

In Equation. (3), B is the encapsulation efficiency of the material. W_S is the drug loading mass of MAF. From this, it can be concluded that the drug loading rate of MAF is shown in Equation. (4).

$$S(\%) = \frac{W_S}{W_{S+T}} \times 100\% \tag{4}$$

In Equation. (4), S is the drug loading rate. W_{S+T} is the total mass of drug loading mass and carrier mass.

Determination of in-vitro thrombin release performance of MnO_2/uPA@pep-Fuco

Then it uses 0, 5 and 10U/mL to prepare thrombin solutions. Further it uses PBS to prepare MAF into a 5mg/mL solution. It absorbs another 3mL into a dialysis bag. The specifications of the dialysis bag are shown in Equation. (5).

$$MWCO = 100kDa \tag{5}$$

This study uses Equation. (5) to dialyze the above thrombin solution and 2mL PBS of dialysate solution is taken out at 0, 8, 16, 24, 36 and 48 hours, respectively. It uses a fluorescence spectrophotometer to measure the fluorescence intensity of the solutions taken out at different times, with an excitation wavelength of 490 nm and an emission wavelength of 525 nm. The formula for calculating the drug release (DR) rate of MAF is shown in Equation. (6).

$$R(\%) = \left(C_n V_0 + V \sum_{i=1}^{n-1} C_1 \right) / W_Z \times 100\% \tag{6}$$

In Equation. (6), C_n and C_1 are the drug concentrations at the time of sampling n and 1, respectively. W_z represents the total mass of drugs in the drug loaded nanosystem. V_o and V are the original volume and sampling volume of dialysate, respectively.

Study on in-vitro precise thrombolysis targeting of MnO_2/uPA@pep-Fuco

After inoculating cells in a 9-well plate with 3×10^5 cells per well for 18 hours, add 0, 2, 6, 12, 18 and 24 μg/mL MPPF nanoparticle culture media to each well and then continue to cultivate for 24 hours. After cultivation, it is washed with PBS in each well to remove free nanoparticles. It then adds 1ml of Calcein-AM staining solution to each well and after staining for 30 minutes, rinse with PBS solution. Then it adds 1mL of PI dye solution to the pores separately and after staining for 3 minutes, rinse the dye solution with PBS solution. Finally, 80% ice ethanol is used to fix the cells for 15 minutes. Cell activity is observed using a fluorescence microscope. When the cell image appears green, it is considered a live cell. When the cell image is red, it is considered dead cells (Witte *et al*., 2020).

Determination of MPPF adhesion to platelets

The platelet material was obtained from venous blood of adult female mice. Platelets are incubated in Calcein-AM staining solution for 20 minutes, followed by washing with PBS to remove excess dye. It cultures the stained platelets in a medium containing 2mol/L $CaCl_2$ solution and 1.5U/mL thrombin for 1 hour and then washes them again with PBS solution. Then it adds 1mL of MPPF dispersion again to the culture dish and incubates at 37°C for 5 hours. After cultivation, the cells are washed again with PBS and stained with Hoechst 33342 solution for 20 minutes. They are then fixed with 4 mol/L paraformaldehyde and examined using a laser confocal scanning microscope.

Measurement of MPPF's removal performance of H_2O_2 from cells

The production of H_2O_2 can promote the formation of blood clots, so the necessary step for drug thrombolysis is to remove H_2O_2 from the cells. The experimental materials are selected from damaged red blood cells induced by oxidized low density lipoprotein (ox LDL). First, it is inoculated with red blood cells at a density of $9*10^3$ cells per well in a 96 well plate and cultured for 12 hours. Then, 0, 30, 60 and 90 μg/mL lipoprotein medium and 120μl of MPPF dispersion are added to the well plate, respectively. Afterwards, the culture continues for 3 hours. Then they take 60% of the supernatant and added H_2O_2 probes to a new 96 well plate. After culturing the well plate at 37°C for 1 hour, the residual H_2O_2 concentration

in the cells is detected using an enzyme-linked immunosorbent assay (Jose *et al*., 2020).

Determination of in-vitro thrombolysis performance of MnO_2/uPA@pep-Fuco

Firstly, thrombus blocks are collected from experimental mice and then placed in a 24 well plate with the same weight for cultivation. The orifice plate is divided into six groups according to the different solutions added to it. The solutions in the first to sixth groups are PBS solution MPPF Solution, free uPA, MAF, MAF +10U/mL thrombin and MUAF +10U/mL thrombin. Then thrombolytic drugs are added to the orifice plate and cultured at 150 rpm at 37°C, recording the weight of the thrombus at different time periods.

***In-vivo precise thrombolysis targeting study of MnO_2/uPA@pep-Fuco* (Construction of a thrombus model in experimental mice)**

The C57BL/6J mice used in the experiment are obtained from Jackson Laboratory. The experimental mice are 6-8 weeks old and weigh approximately 20-25 grams. Mice are housed in standardized animal rooms, with an ambient temperature maintained at 22±1°C and a relative humidity of 50-60%. They undergo a 12 hours light/dark cycle and are provided with sterile drinking water and regular pellet feed. Animals are anaesthetised intraperitoneally with an injection of 12% hydrochloric acid prior to euthanasia. The dose of anaesthesia is 200 g per experimental mice. After anaesthesia, the jugular vein is saturated by isolating it and immersing it in a 10% $FeCl_3$ solution. Subsequently, the damaged area is flushed with PBS solution to remove the $FeCl_3$ solution from the cells. At this point the jugular veins of the experimental rats formed a thrombus model. In this experiment, approximately 20g of female mice are first selected and 12% hydrated chloral solution is injected into the abdomen for anesthesia. Afterwards, the jugular vein is surgically divided and placed in a 10% $FeCl_3$ solution for cell saturation, followed by the use of filter paper to absorb surface moisture. After the experiment, to fulfill the humanitarian endpoint and prevent animals from suffering pain after awakening, all mice were euthanized by cervical dislocation while maintaining deep anesthesia. The complete animal operation process has been reviewed and approved by the Animal Ethics and Use Committee of our unit. Then it uses a syringe to draw PBS solution and rinse the damaged area of the jugular vein twice, removing $FeCl_3$ solution from the cells. At this point, the jugular vein is a thrombus model in experimental mice (Alcantud, 2022).

Vivo thrombolysis determination of MnO_2/uPA@pep-Fuco

The experiment is divided into 6 groups according to the different injection drugs, namely PBS group, MPPF group, free uPA group, MCO/uPA group, MAF group and MUAF group. The different thrombolytic drugs mentioned above are injected into different mice. After 3 hours, the thrombus model of the experimental mice is obtained according to the steps in 2.5.1. It will freeze and slice the obtained model and stain it with hematoxylin dye. It places the stained sections under a fluorescence microscope for observation and calculates the vascular occlusion rate according to Equation. (7).

$$X(\%) = \frac{S_h}{S_z} \times 100\% \tag{7}$$

In Equation. (7), S_h is the cross-sectional area of the thrombus and similarly S_Z for the blood vessel.

Determination of MnO_2/uPA@pep-Fuco's hemolytic performance

In this experiment, MCO and MPPF were prepared in PBS at concentrations of 20, 40, 80 and 100 μg/mL, respectively. Then, 10 μL of platelet solution is taken and placed in the aforementioned dispersion. The platelet solution is placed at 37°C and cultured at a speed of 150rpm for 5 hours. After centrifugation, the supernatant is transferred to a 96-well plate and absorbance is measured at 540 nm using an ELISA reader. It designates PBS solution as a negative control group and ultrapure water as a positive control group. It calculates the hemolytic performance of nanomaterials on the ground of the absorbance value.

$$L(\%) = \frac{As - Anc}{Apc - Anc} \times 100\% \tag{8}$$

In Equation. (8), *As* is the absorbance of the red blood cell sample. *Anc* represents the absorbance of the negative control group. *Apc* represents the absorbance of the positive control group.

Measurement of body weight of experimental mice treated with MnO_2/uPA@pep-Fuco

It divides the experimental mice into five groups according to the type of administration, namely PBS group, MPPF group, free uPA group, MCO/uPA group and MAF group. It injects the above drugs into experimental mice by intravenous injection at a dose of 3.5mg/kg. The experimental period was set to 7 days and the weight changes of the experimental mice were observed and recorded within 7 days. The experimental design of the study aims to systematically compare the thrombolytic effects and safety of different formulations. Therefore, all intervention groups were given a uniform equivalent dose of nanomaterials (3.5 mg/kg) via intravenous injection. The design of a unified intravenous injection dose is mainly aimed at conducting inter group controls to fairly evaluate the potential of MAF nanosystems in improving drug efficacy, enhancing targeting and reducing toxicity.

Determination of biochemical properties of plasma after MnO_2/uPA@pep-Fuco treatment

The mice used in experiment 2.5.4 were selected for plasma collection. It uses a vacuum collection tube to collect blood and extract serum from the blood for

biochemical analysis. The selection of biochemical indicators includes glutamic pyruvic transaminase (GPT), urea, uric acid (UA) and creatinine. The measurement of the above indicators can reflect the liver and kidney function of experimental mice (Gomez *et al*., 2021).

RESULTS

Analysis of characterization results of MnO_2/uPA@pep-Fuco nanodelivery system

According to the discussed method, corresponding nanomaterials can be prepared, and then characterization experiments can be conducted. This study will characterize and analyze the synthesized MAF nanosystem and its corresponding intermediate products and then analyze in-vitro and in- vivo precise thrombolysis performance.

Characterization performance analysis of MnO_2/uPA@ pep-Fuco nanodelivery system

The results show that the overall shape of MnO_2 nanoparticles is spherical and the diameter distribution between different nanoparticles is relatively uniform. The surface of the particles is uneven and the surface of MnO_2 nanoparticles exhibits flower like morphology, which shows that the synthesized MnO_2 flower like nanoparticles have been relatively successful.

Determination of H_2O_2 like enzyme activity of MPF

Fig. 1 shows the activity curve of MPF's H_2O_2 like enzyme. This indicates that the dissolved oxygen content is lower in 0.2mM, 1mM and 100mM H_2O_2 solutions. Dissolved oxygen concentration unit, ppm (Chen L *et al.*, 2024).

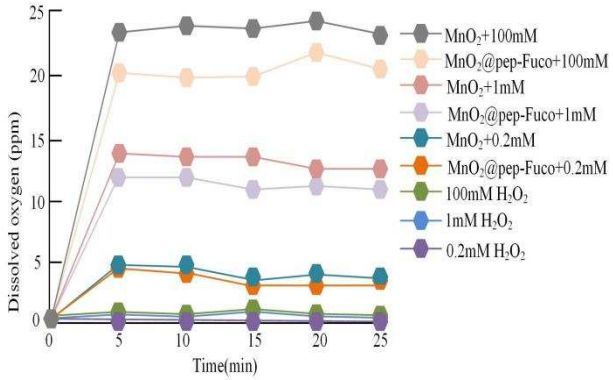

Fig. 1: Class H_2O_2 enzyme activity profile of MnO_2 @pep'-Fuco.

When varying degrees of MnO_2 nanoparticles and MPF nanocomposites are added, the dissolved oxygen gradually increases. At the same concentration, the dissolved oxygen content in the H_2O_2 solution with MnO_2 addition is always higher than that with MPF addition. This is because the PFU composite generates a coating during the synthesis process, reducing the contact area between nanoparticles and H_2O_2 and reducing the dissolved oxygen content.

In-vitro thrombin responsive DR characteristics

Fig. 2 shows the DR of MAF under different concentrations of thrombin. The higher the concentration of thrombin added, the stronger the DR of MAF. In a conventional environment where only PBS exists, the DR effect of MAF is the lowest, with a DR rate of only 55.6% at 50 hours. When there is 10U/mL thrombin in the DR environment, the DR rate of MAF reaches 90.5% at the 50th hour. Therefore, MAF has a high responsive DR ability.

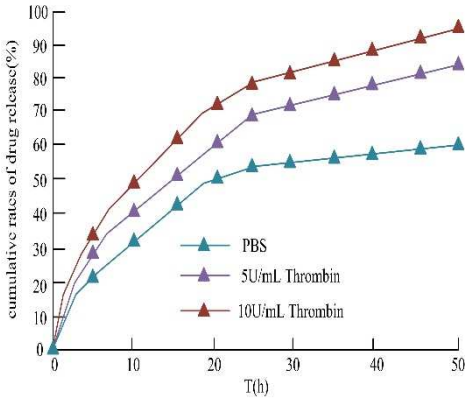

Fig. 2: DR of MnO_2/uPA@pep-Fuco at different concentrations of thrombin states

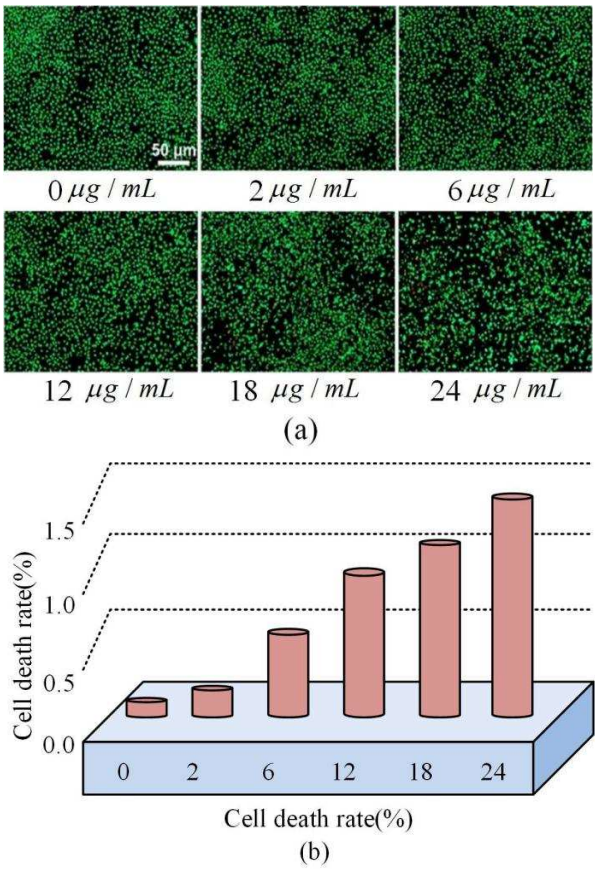

Fig. 3: Evaluates the cell compatibility of MPF nanomaterials. (a): The changes in cell activity at different concentrations of MPPF; (b): Cell activity measurement under MPPF.

Analysis of biochemical performance and thrombolytic ability of MnO_2/uPA@pep-Fuco in-vitro environment

Cell activity measurement under MPPF

Fig. 3 evaluates the cell compatibility of MPF nanomaterials through fluorescence staining images (a) and quantitative statistics (b). The staining results showed that cells treated with 0-24 μg/mL MPPF maintained extensive green live cell fluorescence, and quantitative analysis confirmed that the highest cell mortality rate was only 1.26%. Overall, this nanomaterial has excellent biocompatibility within the experimental concentration range and is suitable as a biological delivery carrier.

Fig. 3 (a) shows the staining of MPPF cells at different concentrations. This indicates that within the concentration range of 0-24μg/ml, cells exhibit green fluorescence over a wide range, indicating a higher activity of the cells.

Fig. 3 (b) shows the cell mortality rate at different concentrations of MPPF. When the concentration of MPPF is 24 μg/ml, the highest cell death rate can reach to 1.26%. This indicates that MPPF nanomaterials have good compatibility within cells and can stably exert thrombolytic properties.

Determination of MnO_2@pep-Fuco adhesion to platelets

The MPPF nanomaterials can fuse a large number of red blood cells and exert effects on them. However, the fusion degree of MCO material on red blood cells is relatively low and the adhesion rate of MPPF nanomaterials is much higher than that of MCO materials, with a maximum adhesion rate of 90.0%.

Measurement of MnO_2@pep-Fuco's removal performance of H_2O_2 from cells

The H_2O_2 clearance effect of MPPF on cells in different states of damage shows that, after induction with ox-LDL and in the absence of MPPF, the intracellular fluorescence intensity of $H_2O_2$is elevated. As the concentration of ox-LOL increases, the fluorescence intensity of H_2O_2 increases, indicating an increase in H_2O_2 content. Upon addition of MPPF, the fluorescence intensity of H_2O_2 is markedly reduced, indicating a corresponding decrease in intracellular H_2O_2 levels. The results indicate that MPPF nanomaterials can effectively reduce H_2O_2 content and eliminate venous thrombosis.

Determination of in-vitro thrombolysis performance of MnO_2/uPA@pep-Fuco

Fig. 4 shows the comparison of thrombus quality and thrombolysis rate after thrombolysis with different materials. Among them, Fig. 4 (a) shows the thrombus mass after thrombolysis with different materials. This indicates that through the delivery system MAF containing drug uPA and the action of drug uPA, the quality of the thrombus gradually decreases. After 5 hours of thrombolysis, the thrombus can ultimately be eliminated. PBS and MPPF without drugs have the worst thrombolytic effect. Fig. 4 (b) shows the thrombolysis rates of different materials. Among them, the thrombolysis rate of PBS and MPPF is only 22.3%, while the thrombolysis rate of uPA and MAF can reach 100%. The thrombolysis rates of MUAF and MAF containing 10U thrombin can reach 48.7% and 49.2%, respectively. Therefore, the MAF delivery system containing uPA can fully exert the efficacy of uPA and dissolve blood clots.

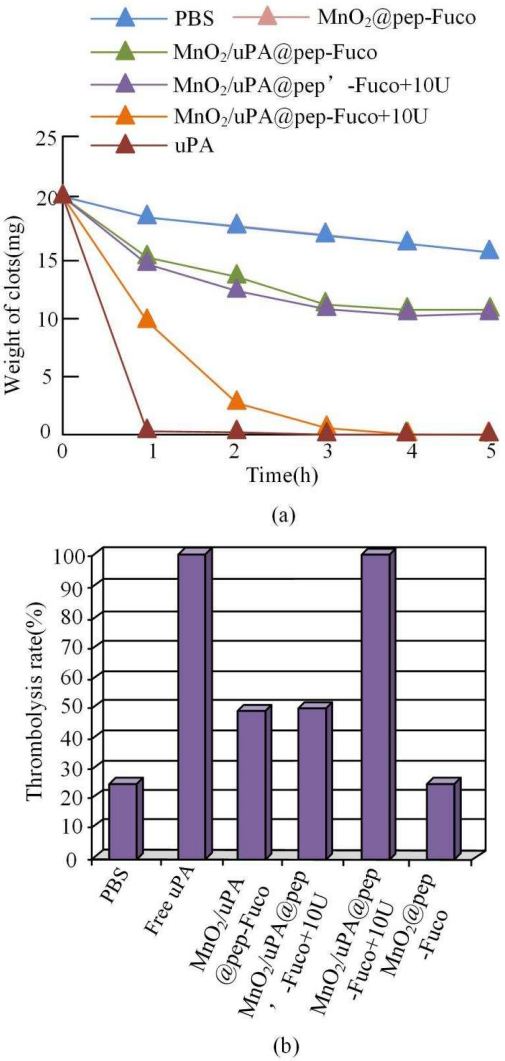

Fig. 4: Comparison of thrombus quality and thrombolysis rate after thrombolysis of different materials. (a) The thrombus mass after thrombolysis with different materials; (b) The thrombolysis rates of different materials.

Accurate in-vivo thrombolysis determination of MnO_2/uPA@pep-Fuco

Fig. 5 shows the comparison of hemolysis rates among different nanomaterials.

Fig. 5 shows the *in-vivo* thrombolysis fluorescence diagram and fluorescence intensity ratio of MAF. Fig. 5 (a) is a schematic diagram of thrombolysis fluorescence using MAF; On the left is a venous thrombosis model

treated with MAF; On the right is a normal venous thrombosis model. The venous thrombosis treated with MAF showed high fluorescence intensity, indicating that nanoparticles can bind and enrich with the thrombus. Fig. 5 (b) shows the fluorescence intensity ratio of the veins on both sides. This indicates that when the thrombolysis time is 30 minutes, the fluorescence intensity ratio of venous thrombosis treated with MAF reaches the highest of 2.7; This indicates that the thrombolysis performance is strongest at this time, and as time goes on, the thrombus gradually clears and the fluorescence intensity gradually decreases. At 90 minutes, the thrombus fluorescence intensity ratio decreased to 2.1.

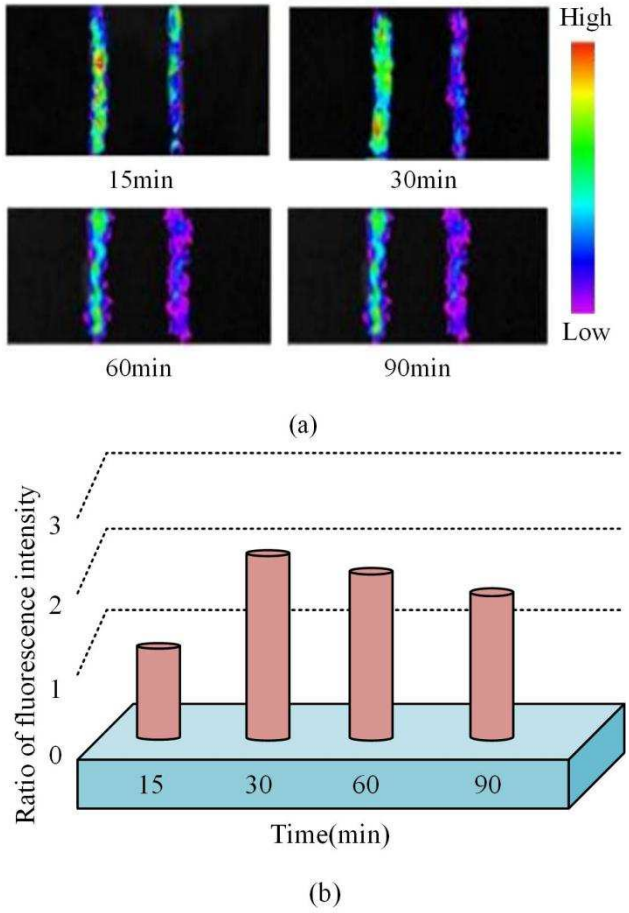

Fig. 5: *In-vivo* thrombolytic fluorescence schematic and fluorescence intensity ratio of MnO_2/uPA@pep-Fuco. (a): Adopt MnO_2@pep-Fuco Processed fluorescence images under arteries; (b):Adopt MnO_2@pep-Fuco Fluorescence intensity ratio under processed arteries

This indicates that when the concentration of added nanomaterials is below 40 μg/mL, the hemolysis rate of MCO is lower than MPPF, indicating stronger compatibility between MCO and blood within this concentration range. When the concentration range is 80 *ug / mL*, the hemolysis rate of MCO exceeds that of MPPF, indicating that at this concentration, MPPF has better compatibility with blood, so the hemolysis degree of nanomaterials is lower. Within 100 *ug / mL*, the highest hemolytic rates achieved by MCO and MPPF are 0.82% and 0.65%, respectively, both below the limit value of 5%. Therefore, the blood compatibility of the above two materials is good and they can effectively exert drug delivery function in venous blood.

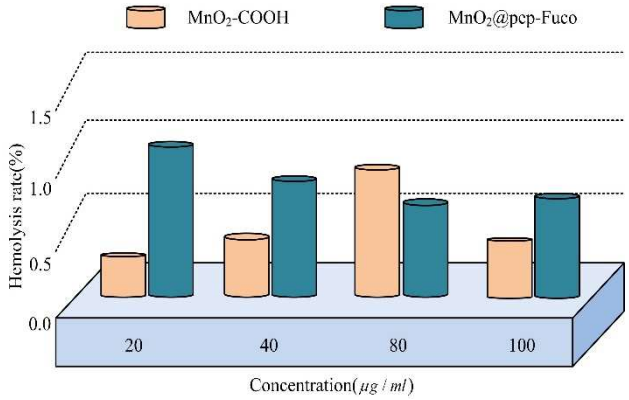

Fig. 6: Comparison of hemolysis rate of different nanomaterials

DISCUSSION

The study compares the thrombolytic efficiency, *in-vivo* targeting and blood compatibility of MAF nanocarriers with the clinical gold standard and verified its performance advantages over rt-PA in targeted sustained release. The addition of positive controls provides a key reference for the clinical translation of nanosystems, confirming their safety. At the same time, the positive control experiment emphasizes the technology's uniqueness by comparing thrombin-responsive release to pH-sensitive carriers. The results of the control experiment are shown in Fig. 5.

Table 1 summarizes the key characterization and performance parameters of the MAF nanodelivery system, and the results show that the prepared MnO_2 nanoparticles have a spherical flower like structure with a PEP Fuco grafting rate of 3.87%. The system exhibits significant H_2O_2 enzyme activity and thrombin responsive drug release characteristics *in-vitro*, with a drug release rate of 90.5% within 50 hours. It also has excellent biocompatibility and blood compatibility, with an *in-vitro* thrombolysis rate of 100%, verifying its potential as an efficient and safe targeted therapy strategy for thrombosis.

The statistical differences in the above results are compared and analyzed and the results are shown in table 2. An independent samples t-test is performed using the PBS group as the control group to compare the differences between the other groups and the PBS group. The table shows that the thrombolysis rates of the MAF group and the free uPA group are significantly higher than those of the other groups ($p<0.001$), while there is no difference between the MPPF group and the PBS group ($p=1.000$).

Table 1: Positive control statistical experiment

Experiment type	Experimental group	New positive control group	Measurement metrics
In-vitro thrombolysis	PBS, MPPF, uPA, MAF, MAF+thrombin, MUAF	Clinical rt-PA (e.g., Alteplase, 10 U/mL)	Thrombus mass reduction rate, thrombolysis rate (%/h)
In-vivo thrombolysis	PBS, MPPF, uPA, MCO/uPA, MAF, MUAF	rt-PA (IV injection, 3.5 mg/kg)	Vascular recanalization rate (%), fluorescence intensity ratio (thrombus/normal)
Hemolysis assay	PBS (negative), ultrapure water (positive)	PEG-coated nanocarriers (80 μg/mL)	Hemolysis rate (%) (absorbance at 540 nm)
Cell viability	MPPF (0–24 μg/mL)	Cisplatin (24 μg/mL)	Cell death rate (%) (Calcein-AM/PI staining)
H_2O_2 scavenging	ox-LDL-damaged cells+MPPF (120 μg/mL)	Catalase (100 U/mL)	H_2O_2 fluorescence intensity (relative)
Drug release	MAF (PBS or thrombin environment)	pH-sensitive polymeric nanoparticles (e.g., PLGA-PEG)	Cumulative release rate (%) (0-50 h)

Table 2: Comparison of statistical differences results

Group	Sample size (n)	Mean ± SD	*T*(t-statistic)	*p* (p-value)	Significance
PBS	6	22.3 ± 3.5%	/	/	/
MPPF	6	22.3 ± 3.5%	0.00	1.025	NS
Free uPA	6	100.0 ± 0.0%	45.71	<0.001	***
MCO/uPA	6	48.7 ± 2.1%	15.23	<0.001	***
MAF	6	100.0 ± 0.0%	45.71	<0.001	***
MAF + 10 U/mL thrombin	6	49.2 ± 1.8%	14.89	<0.001	***

Note: NS indicates no significant difference ($p \geqslant 0.05$). *: $p<0.05$. **: $p<0.01$. ***: $p<0.001$.

Venous thrombosis is a major cardiovascular condition that poses a serious threat to human health. Venous thrombosis is prone to side effects, such as decreased platelet content, during the treatment process. Therefore, developing an intravenous thrombolysis treatment method is of great significance. In the study proposed by Li, L. *et al*., an artificial biomarker nano patrol system was constructed to detect thrombus and thrombin heterogeneity, addressing the shortcomings of traditional weight-based thrombolysis strategies, such as an insufficient reperfusion rate and a high bleeding risk. This system enabled real-time diagnosis and personalized administration of thrombolysis resistance. The system showed a 25% increase in thrombolytic efficiency compared to alteplase in mini pigs and clinical thrombus models, successfully reversing the occlusion of alteplase failed thrombi (Li *et al*., 2025). Wang *et al*. investigated the low reperfusion rate and high bleeding risk associated with traditional thrombolysis. They constructed a multifunctional nanoprobe with a hollow mesoporous silica (HMSN) carrier that was surface-coupled with an RGD peptide and internally co-encapsulated with perfluoropentane (PFP) and indocyanine green (ICG). The probe achieved dual-mode thrombolysis through ultrasound-triggered PFP phase-transition cavitation combined with near-infrared light–activated ICG photothermal synergy. *In-vitro* and small animal arterial embolism models demonstrated that RGD/ICG/PFP@HMSN could effectively target and infiltrate thrombi. Therefore, based on the existing MAF nanoplatform, the current research further introduced the "ultrasound near-infrared (US/NIR) dual-mode" strategy and constructed RGD/ICG/ PFP@HMSN hollow mesoporous silicon nanoprobes: RGD peptides were used to target and penetrate deep into blood clots and PFP was used to achieve ultrasound triggered phase change cavitation mechanical thrombolysis (Wang *et al* 2024). In this study, MAF nanosystems were designed using flower-like MnO_2 as the carrier, functionalized with the targeting peptide pep-Fuco and loaded with uPA. The system integrates the synergistic effects of MnO_2-mediated oxygen supply, RGD-based targeting and uPA-induced fibrinolysis to enable precise thrombus delivery. Experimental results revealed that MAF had a 100% thrombolysis rate within 5 hours, a higher recanalization rate than free uPA, hemolysis of less than 0.82% and was safe for the liver and kidneys. These results verified MAF's high efficiency and low toxicity potential.

CONCLUSION

In order to achieve targeted thrombolysis and enhance treatment safety, this study proposes the preparation of a safe MAF nanso drug delivery system. The preparation process is divided into four steps, namely MnO_2 nanoparticles, PFU composites, MPF nano carriers and MAF nano drug delivery systems. After completing the

preparation of the above materials, their performances are characterized and measured. The experimental results indicate that the prepared MnO_2 nanoparticles has a flower-like structure, which meets the experimental requirements. The grafting rates of PFU and pep'-Fuco are 3.87% and 2.13%, respectively. The PFU complex can increase the dissolved oxygen content in H_2O_2 environment and has certain H_2O_2 like enzyme activity properties. Meanwhile, MAF achieves a DR rate of 90.5% at the 50th hour of the experimental study. *In-vitro*, when the concentration of MPPF is 24, the highest cell death rate is only 1.26% and it has high adhesion to red blood cells, reaching a maximum adhesion rate of 90.0% and the elimination rate of thrombus reaches to 100%. In the *in-vivo* environment, when the thrombolysis time of MAF is 30 minutes, the highest fluorescence intensity ratio of the thrombus model is 2.7. The MPPF carrier can achieve high compatibility in the blood environment, with a maximum hemolysis rate of only 0.65%, where the body weight and biochemical properties of mice after administration are not affected. This indicates that MAF has high safety in the internal environment. However, this study evaluated uPA drug delivery *in-vivo* using experimental mice, while clinical trials in humans will be conducted in the future.

Acknowledgements
The research thanks the support from Zhengzhou University of Industrial Technology and Yuqi BAI Xindian Central Health Center.

Authors' contributions
Dongyan Yin, Yuqi Bai, Ying Wang and Cuiping Zhao conceived the research idea and designed the study. Xiaodong Xiao and Tongtong Li collected the data. Dongyan Yin and Yuqi Bai performed data analysis. All authors discussed the results and wrote the manuscript.

Funding
The research is supported by: Projects of the Ministry of Education's Industry-University Cooperation and Collaborative Education, Construction of a Practical Teaching Mode of Neurorehabilitation Combining Virtual and Real Elements (No. 231107271083604); Projects of the Henan Private Education Association, Research on the Internship Status of Students Majoring in Rehabilitation Therapy in Private Colleges and Universities (No. HNMXL20241835).

Data availability statement
The data used to support the findings of this study are included within the article.

Ethical approval
Ethics Committee approval was obtained from the Institutional Ethics Committee of "College of Medicine, Zhengzhou University of Industrial Technology" (Trial number: 20220612002) to the commencement of the study.

Conflict of interest
The authors declare no conflict of interests.

REFERENCES

Abasian P, Shakibi S, Maniati MS, Khorasani SN and Khuliili S (2021). Targeted delivery, drug release strategies and toxicity study of polymeric drug nanocarriers. *Polym. Adv. Technol.,* **32**(3): 931-944.

Afifi K, Bellanger G, Buyck PJ, Zuurbier SM, Esperon CG, Barboza MA, Costa P, Escudero I, Renard D, Lemmens R, Hinteregger N, Fazekas F, Conde JJ, Giralt-Steinhauer E, Hiltunen S, Arauz A, Pezzini A, Montaner J, Putaala J, Weimar C, Schlamann M, Gattringer T, Tatlisumak T, Coutinho JM, Demaerel P and Thijs V (2020). Features of intracranial hemorrhage in cerebral venous thrombosis. *J. Neurol.,* **267**(11): 3292-3298.

Albertsen IE, Jensen M, Abdelgawwad K, Sogaard M, Larsen TB and Nielsen PB (2021). Characteristics of patients receiving extended treatment after incident venous thromboembolism. Basic Clin. *Pharmacol. Toxicol.* **129**(4): 332-342.

Alcantud JCR (2022). Convex soft geometries. J. Comput. *Cogn. Eng*, **1**(9): 2-12.

Chen L, Wang Y, Zhang X, Li J, Liu Y, Yang H and Zhao K. (2024). TME-activated MnO2/Pt nanoplatform of hydroxyl radical and oxygen generation to synergistically promote radiotherapy and MR imaging of glioblastoma. *J. Nanomed.* **31**(10):11055-11070.

Cheng Y, Lai OM, Tan CP, Panpipat W, Cheong LZ and Shen C (2021). Proline-modified UIO-66 as nanocarriers to enhance candida rugosa lipase catalytic activity and stability for electrochemical detection of nitrofen. *ACS Appl. Mater. Interfaces,* **13**(3): 4146-4155.

Fang MC, Fan D, Sung SH, Witt DM, Schmelzer JR, Williams MS, Yale SH, Baumgartner C and Go AS (2020). Treatment and outcomes of acute pulmonary embolism and deep venous thrombosis: The CVRN VTE study. *Am. J. Med*, **132**(12): 1450-1457.

Gomez K, Laffan M and Bradbury C (2021). Debate: Should the dose or duration of anticoagulants for the prevention of venous thrombosis be increased in patients with COVID-19 while we are awaiting the results of clinical trials. Br. *J. Haematol*, **192**(3): 459-466.

Jose L, Hwang A, Lee C, Shim KH, Song JK, An SSA and Paik HJ (2020). Nitrilotriacetic acid-end-functionalized polycaprolactone as a template for polymer-protein nanocarriers. *Polym. Chem*, **11**(9): 1580-1588.

Kenry YT, She D, Nai M, Valerio VM, Pan Y, Middha E, Lim C and Liu B (2021). Differential collective cell migratory behaviors modulated by phospholipid nanocarriers. *ACS Nano*, **15**(11): 17412-17425.

Li L, Tian H, Wu L, Chen N, Zhang Q, Chen L and Zeng W (2025). Artificial biomarker-based feedback-

regulated personalized and precise thrombolysis with lower hemorrhagic risk. *Sci. Adv*, **11**(3): 377-378.

Li W, Kessinger CW, Orii M, Lee H, Wang L, Weinberg I, Jaff MR, Reed GL, Libby P, Tawakol A, Henke PK and Jaffer FA (2021). Time-restricted salutary effects of blood flow restoration on venous thrombosis and vein wall injury in mouse and human subjects. *Circulation*, **143**(12): 1224-1238.

Lin F, Xie Y, Deng T and Zink JI (2021). Magnetism, ultrasound and light-stimulated mesoporous silica nanocarriers for theranostics and beyond. J. *Am. Chem*. Soc., **143**(16): 6025-6036.

Ma X, Liang N, Qin L, Huo W and Li Y (2024). Damage of polyethylene microplastics on the intestine multilayer barrier, blood cell immune function and the repair effect of *Leuconostoc mesenteroides* DH in the large-scale loach (*Paramisgurnus dabryanus*). *Fish Shellfish Immunol*, **147**: 109460-109461.

Miao Y, Yang Y, Guo L, Chen M, Zhou X, Zhao Y, Nie D, Gan Y and Zhang X (2022). Cell membrane-camouflaged nanocarriers with biomimetic deformability of erythrocytes for ultralong circulation and enhanced cancer therapy. *ACS Nano*, **16**(4): 6527-6540.

Mittal A, Kumar S, Singh P, Gupta R and Sharma S. (2020). Fabrication of oligo-glycerol based hydrolase responsive amphiphilic nanocarriers. *Polym. Adv*, **31**(6): 1208-1217.

Mittal A, Singh AK, Kumar A, Parmanand KA, Haag R and Sharma SK (2020). Fabrication of oligo-glycerol based hydrolase responsive amphiphilic nanocarriers. *Polym. Adv. Technol*, **31**(6): 1208-1217.

Oshiro-Júnior JA, Rodero C, Hanck-Silva G, Sato MR, Alves RC, Eloy JO and Chorilli M (2020). Stimuli-responsive drug delivery nanocarriers in the treatment of breast cancer. *Curr. Med. Chem*, **27**(15): 2494-2513.

Powell M, Villers KT, Schwarz K, David C and Toby T (2021). ASingle-center retrospective evaluation of the use of oral factor xa inhibitors in patients with cerebral venous thrombosis. *Ann*. *Pharmacother*, **55**(3): 286-293.

Schmitt S, Huppertsberg A, Klefenz A, Kaps L, Mailänder V, Schuppan D, Butt H, Nuhn L and Koynov K (2022). Fluorescence correlation spectroscopy monitors the fate of degradable nanocarriers in the blood stream. *Biomacromolecules*, **23**(3): 1065-1074.

Wang Z, Jiang N, Jiang Z, Wang H, Guo Y, Zhong F and Hu B (2024). Dual-mode nanoprobe strategy integrating ultrasound and near-infrared light for targeted and synergistic arterial thrombolysis. *J. Nanobiotechnol*, **22**(1): 311-312.

Wilson BK, Sinko PJ and Prud'Homme RK (2021). Encapsulation and controlled release of a camptothecin prodrug from nanocarriers and microgels: Tuning release rate with nanocarrier excipient composition. *Mol. Pharm*, **18**(3): 1093-1101.

Witte TMD, Wagner AM, Fratila-Apachitei LE, Zadpoor AA and Peppas NA (2020). Immobilization of nanocarriers within a porous chitosan scaffold for the sustained delivery of growth factors in bone tissue engineering applications. J. *Biomed. Mater. Res. A*, **108**(5): 1122-1135.

Xu Y, Hul MV, Suriano F, Preat V and Beloqui A (2019). Novel strategy for oral peptide delivery in incretin-based diabetes treatment. *Gut*, **69**(5): 911-919.

Zajdel A, Wilczok A, Jelonek K, Kaps A, Musial-kulik M and Kasperczyk J (2021). Cytotoxic effect of targeted biodegradable epothilone B and rapamycin co-loaded nanocarriers on breast cancer cells. *J. Biomed. Mater. Res*, **109**(9): 1693-1700.

Zhang H, Li X, Wang C, Liu Y, Chen J, Yang M and Wu Z (2025). Thrombin-responsive and sequential targeted nanoplatform for synergistic *Thrombolysis ACS Appl. Mater. Interfaces*. **17**(11): 16696-16607.

Zhou J, Wang Y, Li X, Zhang C and Liu H (2019). Template-assisted synthesis of hollow manganese dioxide nanoparticles for enhanced drug delivery. *J. Mater. Chem*, **7**(12): 2054-2061.

Zhou Y, Li K, Li F, Han S, Wang Y, Li X and Zhan Y (2019). Doxorubicin and ABT-199 coencapsulated nanocarriers for targeted delivery and synergistic treatment against hepatocellular carcinoma. *J. Nanomater*, **3**(1): 1-13.